

# Decentralized Domain Generalization with Style Sharing: Formal Model and Convergence Analysis

Shahryar Zehtabi<sup>a</sup>, Dong-Jun Han<sup>b</sup>, Seyyedali Hosseinalipour<sup>c</sup>, Christopher G. Brinton<sup>a</sup>  
<sup>a</sup> Purdue University, <sup>b</sup> Yonsei University, <sup>c</sup> University at Buffalo — SUNY

**Abstract**—Much of federated learning (FL) focuses on settings where local dataset statistics remain the same between training and testing. However, this assumption often does not hold in practice due to distribution shifts, motivating the development of domain generalization (DG) approaches that leverage source domain data to train models capable of generalizing to unseen target domains. In this paper, we are motivated by two major gaps in existing work on FL and DG: (1) the lack of formal mathematical analysis of DG objectives; and (2) DG research in FL being limited to the star-topology architecture. We develop Decentralized Federated Domain Generalization with Style Sharing (STYLEDDG), a decentralized DG algorithm which allows devices in a peer-to-peer network to achieve DG based on sharing style information inferred from their datasets. Additionally, we provide the first systematic approach to analyzing style-based DG training in decentralized networks. We cast existing centralized DG algorithms within our framework, and employ their formalisms to model STYLEDDG. We then obtain analytical conditions under which convergence of STYLEDDG can be guaranteed. Through experiments on popular DG datasets, we demonstrate that STYLEDDG can obtain significant improvements in accuracy across target domains with minimal communication overhead compared to baseline decentralized gradient methods.

**Index Terms**—Decentralized Federated Learning, Domain Generalization

## I. INTRODUCTION

Federated learning (FL) enables multiple edge devices to collaboratively train a machine learning (ML) model using data stored locally on each device [1]. Existing conventional “star-topology” FL methods rely on a central server to conventionally sent from the clients [2]. However, in decentralized networks, a central server may not always be available to conduct model aggregations [3]. Motivated by this, recent research has investigated decentralized federated learning (DFL), in which edge devices iteratively communicate their model parameters with their one-hop neighbors after completing their local model training [4]. While synchronization among the participating edge devices in conventional FL is readily guaranteed through the aggregation at the end of each training round, DFL algorithms need to incorporate a cooperative consensus strategy to their learning process so that devices gradually learn the same model [5].

When training ML models via FL/DFL, it is typically assumed that the test data is drawn from the same probability distribution as the training data [6]. However, this assumption does not always hold; in many real-world applications, a distribution shift can occur between the training set (source) and the test set (target) [7]. For example, consider a network of autonomous vehicles [8] aiming to improve their image

classification models using DFL. As these devices are driven mostly during the morning and the afternoon, they mostly contain images in daylight (source domains), while their goal is to train a generalized model capable of classifying images taken at night (target domain) as well. It has been shown that ML algorithms can drastically fail to achieve generalization to such unseen target domains without making any special adjustments to their training processes [9]. Domain generalization (DG) aims to mitigate this issue, with the goal of preventing performance degradation under such distribution shifts [6].

Due to the practical importance of enabling DG in FL settings, recent research has focused on federated domain generalization (FDG) [10], where DG algorithms are designed to operate in a distributed manner across edge devices. FDG introduces further challenges compared to centralized DG, primarily due to the limited number of source domains accessible to each device [11]. In FDG, in addition to label heterogeneity across devices, source heterogeneity must be also considered, further complicating the goal of achieving DG [12]. For instance, in the previously mentioned example, one device may contain images collected in the morning, while another holds images taken in the afternoon, yet the constructed global model is expected to make reliable predictions on night-time images.

**Research objectives.** A large class of DG algorithms are *style-based*, with style statistics estimated from the source dataset and explored for generalization to the target. These works, whether for centralized training [6] or star-topology FL [10], lack a concrete mathematical formulation of the objective function being optimized to train domain-invariant models. Furthermore, the studied DG algorithms in FL are constrained by their star-topology networks, and cannot be readily extended to arbitrary decentralized networks. In this paper, we present one of the first style-based decentralized FDG algorithms, called *Decentralized Federated Domain Generalization with Style Sharing* (STYLEDDG), in which edge devices communicate style information of their local datasets with their one-hop neighbors so that collectively they can train ML models that generalize well to unseen domains. Our STYLEDDG algorithm, illustrated in Fig. 1, is inspired by the work in [13], where the authors present an FDG algorithm called StableFDG. Different than [13], STYLEDDG is a fully decentralized DG algorithm, and does not add any further oversampling or attention layers as in StableFDG. The computation overhead of StableFDG is at least doubled compared to its analogous models, due to its oversampling step and the added attention layer, and this in turn obstructs our

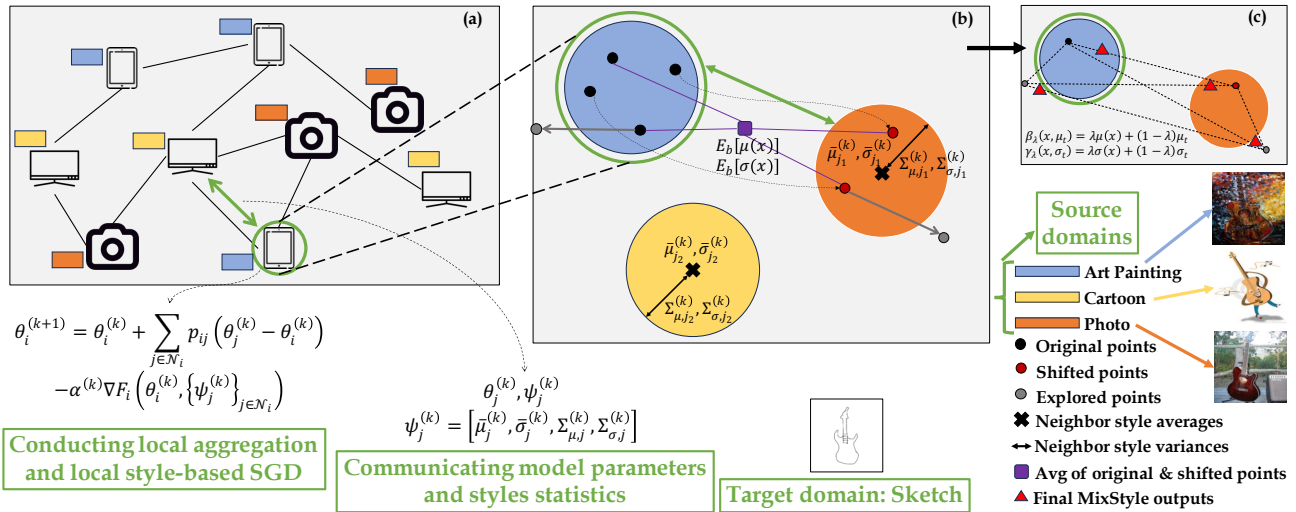


Fig. 1: Proposed DDG methodology. (a) A decentralized network comprised of  $m = 9$  devices, with each device having data from one of three domains (painting, cartoon, photo). The performance of DDG is evaluated on the fourth domain (sketch). (b) In STYLEDGD, each device first uses the style statistics of a neighbor for style shifting (getting to red dots from the black ones) for a portion its batch size. Then it concatenates the original plus the shifted points and chooses a new portion of them to do style extrapolation with and generate new styles (grey dots). The circles shown illustrate the style space at the output of a neural network layer. (c) After randomly shifting a portion of the points in the original mini-batch to a new style, and then randomly extrapolating a new portion of the outputs, we are left with a new set of styles with size equal to the original mini-batch. In STYLEDGD, we use these new points (red triangles) and apply MixStyle within them.

understanding of its style exploration strategy in achieving DG performance. Lastly, our other main contribution is to provide the first formal modeling of style-based DG training, both for well-known DG methods and for STYLEDGD.

**Contributions.** Our key contributions are as follows:

- We present STYLEDGD, one of the first fully decentralized domain generalization (DDG) algorithms. In our setup, devices in a decentralized system aim to achieve DG without having any information about the whole network graph, and can only communicate with their one-hop neighbors, unlike in star-topology FL. Specifically, each device in DDG trains an ML model locally using its local dataset, and then it exchanges (i) its ML model parameters and (ii) style statistics of its current batch with its neighbors (see Fig. 1-(a)). Afterward, each device employs the received style statistics from its neighbors to explore the style space more effectively for DG (see Fig. 1-(b)).
- Among all style-based DG methods, for the first time in the literature, we provide a systematic approach to mathematically formulate the training objective function and optimization procedure. As the operations of style-based methods have commonalities, we first derive a set of concrete formulations for well-known style-based DG methods. These generalized formulations lay the groundwork for formal modeling of future methods in this emerging field, applicable to both centralized and distributed/federated network settings.
- Exploiting the above-mentioned analytical framework, we present a formal modeling of the objective function of STYLEDGD and conduct convergence analysis, enabling us to provide one of the first convergence guarantees among all style-based DG papers. Our results illustrate

that under certain conditions on the employed ML model, the smoothness of local loss functions can be guaranteed for each device. Consequently, this ensures that all devices collectively converge to the same optimal model.

- Through experiments on two DG datasets, we demonstrate that our STYLEDGD method outperforms other centralized/federated DG methods applied in a decentralized learning setting, in terms of the final achievable test accuracy on unseen target domains.

## II. RELATED WORK

**Decentralized federated learning (DFL).** A recent line of work has considered FL over non-star topologies. This includes semi-decentralized FL [14], [15], which groups the devices into several subnetworks, with devices conducting intra-subnet communications before exchanging their model parameters with the centralized server. Fog learning generalizes this to multi-layer hierarchies between the edge devices and the backbone servers [16]. DFL is at the extreme end of this spectrum, where communication is entirely peer-to-peer, with the goal of iteratively updating and exchanging models over the device graph to arrive at an optimal ML model [17]–[21]. Nevertheless, currently there does not exist any DFL algorithm which is tailored for DG. In this paper, we propose a DG methodology tailored to the DFL network setting, leading to one of the first style-based DDG algorithms in the literature.

**Domain generalization (DG).** DG aims to achieve generalization to out-of-distribution data from unseen target domains using distinct source domain data for training (see [6], [9] for recent surveys). While various classes of ML methods can be considered DG – like meta-learning [22], [23], self-supervised learning [24], regularization [25] and domain alignment [26], [27] – our focus in this paper is on

the family of *feature augmentation, style-based* methods for DG. In particular, algorithms like MixStyle [28] and DSU [29] achieve DG via feature-level augmentation, where the styles of images are explored beyond the distribution of styles that exist within the source domains. In the core of these algorithms, they employ AdaIN [30] (adaptive instance normalization) to explore new features/styles during training. Compared to other DG methods, an advantage of style-based methods is that they do not require the domain labels to be known [13].

Despite the notable progress in this domain, a major drawback of current research on DG is the lack of concrete formulations for objective functions. Thus, convergence guarantees for these methods have remained elusive. We fill this gap by rigorously formulating the optimization procedures of prior well-known DG methods and our approach, and by providing a convergence analysis in decentralized network settings.

**Federated domain generalization (FDG).** Data heterogeneity is a notable challenge in FL, as the distribution of data among devices are non-IID [31]. This challenge becomes even more prominent when the distribution of test data is different than the distribution of training data available in devices, motivating the development of FDG algorithms. In this direction, FedBN [32] proposed to not average the local batch normalization layers to alleviate the feature shift problem. In StableFDG [13], each device uses one of the styles of other devices received from the server, and extrapolates the region outside the existing style domains to achieve generalization.

However, existing FDG methods [33]–[36] are tailored for conventional star-topology FL settings. DFL introduces novel challenges due to the need to incorporate peer-to-peer consensus mechanisms. In this paper, we present one of the first decentralized domain generalization (DDG) algorithms. Furthermore, we are unaware of any style-based DG algorithm with concrete convergence analysis. Our work thus fills an important gap through our formal modeling of the DG objective functions, which not only helps us gain insights to the theoretical implications of our proposed methodology, but also lays the foundation for rigorous formulation and convergence analysis of future style-based DG methods [37], [38].

### III. STYLE-BASED DOMAIN GENERALIZATION

We begin with preliminaries in Sec. III-A. Then in Sec. III-B we discuss the problem formulation. Finally, we provide a novel mathematical formulation for the objective functions of two centralized DG algorithms in Sec. III-C, which we later use in Sec. IV to formulate our STYLEDG algorithm.

#### A. Preliminaries

1) *Notation:* We denote the model parameters of a neural network with dimension  $n \in \mathbb{Z}^+$  by  $\theta \in \mathbb{R}^n$ . Let us partition the model  $\theta$  to  $L \in \mathbb{Z}^+$  partitions. We use the notation  $\theta_\ell \subset \theta$  with  $\ell = 1, \dots, L$  as the sub-model with the model parameters of only partition  $\ell$  of the model  $\theta$ . Thus, we will have  $\theta = [\theta_1^T \dots \theta_L^T]^T$ . We focus much of our presentation on convolutional neural networks (CNNs), given their widespread use in DG methods over vision/image applications. As an

example, Fig. 2-(b) shows how a ResNet model [39] can be partitioned by its convolutional blocks.

We abstract the operations applied at the end of each layer  $\ell$  as  $h_{\theta_\ell}(\cdot)$ , giving the final output of the CNN for an input  $x$  as  $(h_{\theta_L} \circ \dots \circ h_{\theta_1})(x)$ , where  $\circ$  denotes the composition operator. Let us denote the loss function as  $\mathcal{L}(h_\theta(x), y)$  which takes the predicted outputs  $h_\theta(x)$  and true labels  $y$  and calculates the loss based on them. Also, letting  $\tilde{\mathcal{P}}(\cdot)$  denote the power set of a given set, we define a function  $\mathcal{P}$  which takes a positive integer input  $L \in \mathbb{Z}^+$  and outputs  $\mathcal{P}(L) = \tilde{\mathcal{P}}(\{\ell : 1 \leq \ell \leq L\})$  with cardinality  $|\mathcal{P}(L)| = 2^L$ . Finally, let  $\mathfrak{S}_{\mathcal{I}} = \text{Permute}(\mathcal{I})$  be the set of all possible permutations of set  $\mathcal{I}$ .

2) *AdaIN:* Adaptive instance normalization (AdaIN) [30] plays a key role in style-based DG methods by enabling style transfers. This technique removes the style information of a data sample and replaces it with the style of another sample. Specifically, the AdaIN process can be written as follows:

$$\text{AdaIN}(x, \mu_t, \sigma_t) = \sigma_t \cdot \frac{x - \mu(x)}{\sigma(x)} + \mu_t, \quad (1)$$

where the tensor  $x \in \mathbb{R}^{B \times C \times H \times W}$  is taken to be a batch of size  $B$  at a specific layer of the CNN with a channel dimension of  $C$ , width  $W$  and height  $H$ , and  $x_{b,c,h,w}$  denotes the value at the indexed dimensions. Furthermore,  $\mu_t, \sigma_t \in \mathbb{R}^{B \times C}$  are the statistics of a target style to which we want to shift the style of  $x$  to, and the instance-level mean and standard deviation  $\mu(x), \sigma(x) \in \mathbb{R}^{B \times C}$  for each channel are calculated as

$$\begin{aligned} \mu(x)_{b,c} &= \frac{1}{HW} \sum_{h=1}^H \sum_{w=1}^W x_{b,c,h,w}, \\ \sigma^2(x)_{b,c} &= \frac{1}{HW} \sum_{h=1}^H \sum_{w=1}^W (x_{b,c,h,w} - \mu(x)_{b,c})^2 + \eta, \end{aligned} \quad (2)$$

where  $\mu(x) = [\mu(x)_{b,c}]_{\substack{1 \leq b \leq B, \\ 1 \leq c \leq C}}$ ,  $\sigma(x) = [\sigma(x)_{b,c}]_{\substack{1 \leq b \leq B, \\ 1 \leq c \leq C}}$ , and  $\eta > 0$  is a small value for numerical stability. We note that the AdaIN function in Eq. (1) first normalizes the style of  $x$  by calculating  $(x - \mu(x))/\sigma(x)$ , and then scales the result by  $\sigma_t$  and shifts it by  $\mu_t$  to move it to a desired target style.

3) *Higher-order statistics:* After computing the mean  $\mu(x)$  and standard deviation  $\sigma(x)$  for a given batch  $x$  as its first-order style statistics, we can further extract second-order style statistics  $\Sigma_\mu^2(x), \Sigma_\sigma^2(x) \in \mathbb{R}^C$  as the variance of each of them:

$$\begin{aligned} \Sigma_\mu^2(x)_c &= \frac{1}{B} \sum_{b=1}^B (\mu(x)_{b,c} - \mathbb{E}_b[\mu(x)_{b,c}])^2 + \eta, \\ \Sigma_\sigma^2(x)_c &= \frac{1}{B} \sum_{b=1}^B (\sigma(x)_{b,c} - \mathbb{E}_b[\sigma(x)_{b,c}])^2 + \eta, \end{aligned} \quad (3)$$

where  $\Sigma_\mu^2(x) = [\Sigma_\mu^2(x)_c]_{1 \leq c \leq C}$ ,  $\Sigma_\sigma^2(x) = [\Sigma_\sigma^2(x)_c]_{1 \leq c \leq C}$ .

#### B. Problem Formulation

We consider a decentralized device-to-device (D2D) network represented by a graph  $\mathcal{G} = (\mathcal{M}, \mathcal{E})$ , where  $\mathcal{M} = \{1, \dots, m\}$  is the set of devices/nodes, and  $\mathcal{E}$  indicates the set of communication edges between the devices. We assume that the graph is connected, and define the set of one-hop

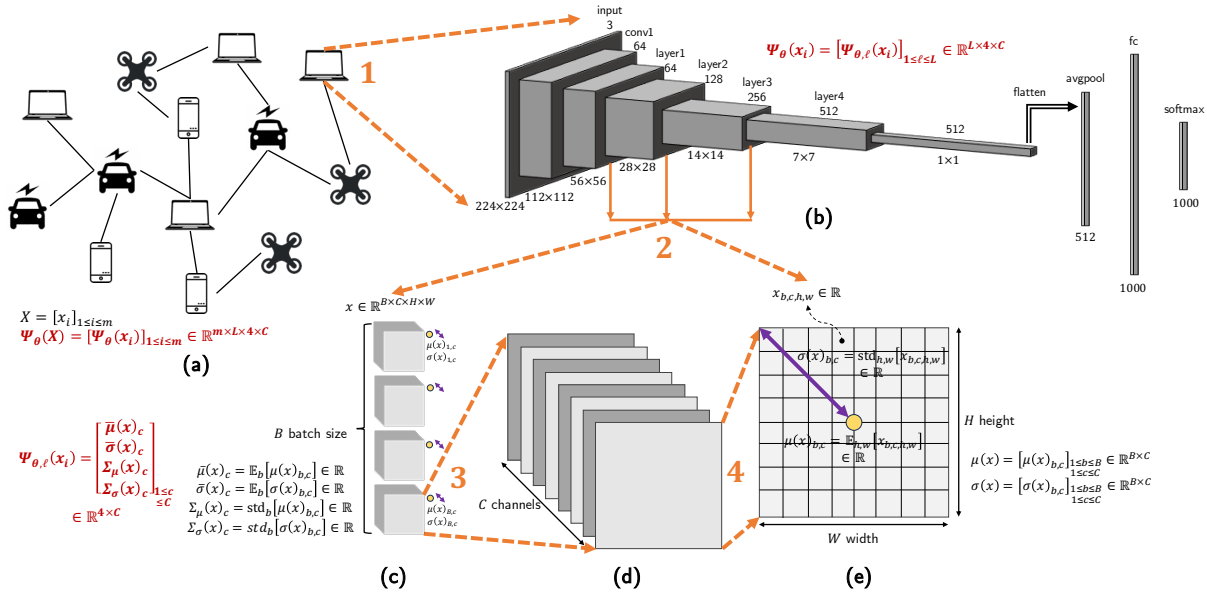


Fig. 2: Illustration of style statistics. (a) A decentralized network with devices having access to data from only a single domain. (b) An overview of the ResNet18 model [39] as an example model at each device, where the number of channels and output size of each block are indicated. We visualize the blocks/layers that STYLEDDG is applied to, which correspond to layers where we extract style statistics from. (c) Illustrates the outputs of a particular layer for all instances in the batch of size  $B$ . The style statistics that each device shares with its neighbors are obtained in the batch-level as shown. (d) For a given instance in the batch, the style statistics are calculated for each channel separately. (e) The  $\mu$  and  $\sigma$  of style statistics are computed based on the mean and standard deviation of the layer outputs.

neighbors of a device  $i \in \mathcal{M}$  as  $\mathcal{N}_i$ . In DFL [12], [15], device  $i$  maintains an ML model  $\theta_i$ , and engages in (i) local model updates and (ii) inter-device communications to train a globally optimal model. Also, each device  $i$  contains a local dataset  $\mathcal{D}_i = \{(x_i, y_i, d_i)_k\}_{k=1}^{|\mathcal{D}_i|}$  where the  $(x_i, y_i, d_i)_k$  pair indicates the  $k$ th data point with input features  $x_i$ , label  $y_i$  and, unique to the DG setting, domain  $d_i$ . For example, in the well-known PACS dataset [40], each domain corresponds to a visual style, namely, art painting, cartoon, photo, or sketch.

In our decentralized DG (DDG) setting, the goal is to train a domain-invariant global model  $\theta$  over the device network  $\mathcal{G}$  that generalizes well to unseen domains. In the PACS dataset example, a global model trained on art painting, cartoon, and photo domains should generalize well to the sketch domain, despite the absence of sketch data and a central model aggregation server during the training process.

### C. Formal Modeling of Centralized DG

In this section, we provide the first formal models of the MixStyle [28] and DSU [29] algorithms for centralized DG. Note that the original papers and subsequent works do not present any such objective functions. This serves as a precursor to developing our STYLEDDG algorithm in Sec. IV-B.

1) MixStyle [28]: In MixStyle, the style space of the CNN layers are explored through convex combinations of the existing styles, thereby exposing the model to styles beyond the existing ones in the training batch. For a given instance  $x$  and target style statistics  $\mu_t$  and  $\sigma_t$ , the MixStyle operation employs AdaIN from Eq. (1) as

$$\text{MixStyle}(x, \mu_t, \sigma_t) = \text{AdaIN}(x, \beta_\lambda(x, \mu_t), \gamma_\lambda(x, \sigma_t)), \quad (4)$$

where the shifting and scaling parameters are defined as

$$\begin{aligned} \beta_\lambda(x, \mu_t) &= \lambda\mu(x) + (1 - \lambda)\mu_t, \\ \gamma_\lambda(x, \sigma_t) &= \lambda\sigma(x) + (1 - \lambda)\sigma_t, \end{aligned} \quad (5)$$

respectively, and  $\lambda$  is the mixing coefficient. The original paper [28] applies MixStyle to all convolutional blocks except the last one for ResNet ( $L = 3$ ). They sample  $\lambda$  for each layer from the Beta distribution  $\mathbb{P}_\lambda = \text{Beta}(0.1, 0.1)$ . Additionally, for each layer  $\ell = 1, \dots, L$ , they assign a probability  $p_\ell = 0.5$  of applying MixStyle to layer  $\ell$ .

**Our formal objective model.** We can formally model MixStyle's objective function. For a mini-batch  $x$  of size  $B$ , MixStyle's loss function with random shuffling is given as

$$F(\theta) = \sum_{\pi \in \mathcal{P}(L)} \left( \prod_{\ell \in \pi} p_\ell \right) \mathbb{E}_{\substack{(x,y) \sim \mathbb{P}_D \\ \{I_\ell \in \mathfrak{S}_B\}_{\ell \in \pi} \\ \{\lambda_\ell \sim \mathbb{P}_\lambda\}_{\ell \in \pi}}} \left[ \mathcal{L}(\hat{h}_{\theta, \{I_\ell, \lambda_\ell\}_{\ell \in \pi}}(x), y) \right], \quad (6)$$

where  $\mathbb{P}_D$  denotes the probability distribution of data in the source domains and  $\mathfrak{S}_B$  is the set of all possible permutations of the set  $\mathcal{B} = \{1, \dots, B\}$ . In other words, [28] applies the MixStyle strategy to the outputs of the model's layer  $\ell$  with a probability  $p_\ell$ , so that the overall model is modified as

$$\hat{h}_{\theta, \{I_\ell, \lambda_\ell\}_{\ell \in \pi}}(x) = (\hat{h}_{\theta_L, I_L, \lambda_L} \circ \dots \circ \hat{h}_{\theta_1, I_1, \lambda_1})(x), \quad (7)$$

in which  $\hat{h}_{\theta_\ell, I_\ell, \lambda_\ell} = h_{\theta_\ell}$  if  $\ell \notin \pi$ . If  $\ell \in \pi$ , we define  $x_m = [x_k]_{k \in I_\ell}^T$  as a permuted version of the mini-batch  $x$  based on the shuffled indices  $I_\ell$ , and then the MixStyle update that occurs at that layer can be defined using Eq. (4) as

$$\hat{h}_{\theta_\ell, I_\ell, \lambda_\ell}(x) = \text{MixStyle}(h_{\theta_\ell}(x), \mu(h_{\theta_\ell}(x_m)), \sigma(h_{\theta_\ell}(x_m))), \quad (8)$$

Note that the MixStyle layer is taking the model outputs for mini-batch  $x$  and the style statistics  $\mu(\cdot)$  and  $\sigma(\cdot)$  of the permuted mini-batch  $x_m$  from Eq. (2) for feature augmentation.

2) DSU [29]: DSU is another centralized DG algorithm where the style space of the CNN layers are explored by adding a Gaussian noise to the existing styles. For a given instance  $x$  and target higher-order style statistics  $\Sigma_{\mu,t}$  and  $\Sigma_{\sigma,t}$ , the DSU operation invokes AdaIN from Eq. (1) as

$$\text{DSU}_{\epsilon_\mu, \epsilon_\sigma}(x, \Sigma_{\mu,t}, \Sigma_{\sigma,t}) = \text{AdaIN}(x, \beta_{\epsilon_\mu}(\mu(x), \Sigma_{\mu,t}), \gamma_{\epsilon_\sigma}(\sigma(x), \Sigma_{\sigma,t})), \quad (9)$$

where the shifting and scaling parameters are defined as

$$\beta_{\epsilon_\mu}(\mu, \Sigma_{\mu,t}) = \mu + \epsilon_\mu \Sigma_{\mu,t}, \quad \gamma_{\epsilon_\sigma}(\sigma, \Sigma_{\sigma,t}) = \sigma + \epsilon_\sigma \Sigma_{\sigma,t}, \quad (10)$$

respectively, and  $\epsilon_\mu$  and  $\epsilon_\sigma$  follow a Normal distribution. Specifically, [29] applies DSU to all convolutional blocks alongside the first convolutional layer and the max pooling layer of a ResNet model ( $L = 6$ ). The exploration coefficients  $\epsilon_{\mu,\ell}, \epsilon_{\sigma,\ell}$  are sampled for each layer  $\ell$  from distributions  $\mathbb{P}_{\epsilon_\mu}, \mathbb{P}_{\epsilon_\sigma}$  set as  $\mathbb{P}_{\epsilon_\mu} = \mathbb{P}_{\epsilon_\sigma} = \mathcal{N}(0, 1)$ , i.e., unit Gaussian. As in MixStyle, the probability of applying DSU to each layer  $\ell = 1, \dots, L$  is set to  $p_\ell = 0.5$ .

**Our formal objective model.** For a mini-batch  $x$  of size  $B$ , the loss function of DSU can be formalized as

$$F(\theta) = \sum_{\pi \in \mathcal{P}(L)} \left( \prod_{\ell \in \pi} p_\ell \right) \mathbb{E}_{\substack{(x,y) \sim \mathbb{P}_D \\ \{\epsilon_{\mu,\ell} \sim \mathbb{P}_{\epsilon_\mu}\}_{\ell \in \pi} \\ \{\epsilon_{\sigma,\ell} \sim \mathbb{P}_{\epsilon_\sigma}\}_{\ell \in \pi}}} \left[ \mathcal{L}(h_{\theta, \{\epsilon_{\mu,\ell}, \epsilon_{\sigma,\ell}\}_{\ell \in \pi}}(x), y) \right]. \quad (11)$$

In essence, this method applies its DSU strategy to the outputs of the model's layer  $\ell$  with a probability  $p_\ell$ , so that the overall model is modified as

$$\hat{h}_{\theta, \{\epsilon_{\mu,\ell}, \epsilon_{\sigma,\ell}\}_{\ell \in \pi}}(x) = (\hat{h}_{\theta_{L, \epsilon_{\mu,L}, \epsilon_{\sigma,L}}} \circ \dots \circ \hat{h}_{\theta_{1, \epsilon_{\mu,1}, \epsilon_{\sigma,1}}})(x), \quad (12)$$

in which  $\hat{h}_{\theta_{\ell, \epsilon_{\mu,\ell}, \epsilon_{\sigma,\ell}}} = h_\theta$  if  $\ell \notin \pi$ . If  $\ell \in \pi$ , then the DSU update that occurs at that layer can be defined as

$$\hat{h}_{\theta_{\ell, \epsilon_{\mu,\ell}, \epsilon_{\sigma,\ell}}}(x) = \text{DSU}_{\epsilon_{\mu,\ell}, \epsilon_{\sigma,\ell}}(h_{\theta_\ell}(x), \Sigma_\mu(h_{\theta_\ell}(x)), \Sigma_\sigma(h_{\theta_\ell}(x))), \quad (13)$$

where the DSU layer takes the model outputs for mini-batch  $x$  and the higher-order style statistics  $\Sigma_\mu(\cdot)$  and  $\Sigma_\sigma(\cdot)$  of that batch as calculated in Eq. (3) to conduct feature augmentation.

The loss function formulations we derived in Eqs. (6) and (11) provide us with compact representations that will enable us to formally model our STYLEDG algorithm in Sec. IV. We observe that minimizing Eqs. (6) and (11) results in learning style-invariant model parameters for all different combinations of the layers/blocks in the CNN, by taking a convex combination of the styles (for MixStyle) and adding Gaussian noise to the styles of each layer (for DSU).

#### IV. DECENTRALIZED STYLE-BASED DG

In Sec. IV-A, we present the steps of our STYLEDG decentralized DG methodology, summarized in Alg. 1. Then, we proceed to formally model STYLEDG in Sec. IV-B.

##### A. STYLEDG Algorithm

1) *Gradient Descent and Consensus Mechanism:* In our decentralized network setup, each device  $i \in \mathcal{M}$  maintains a local model  $\theta_i^{(k)}$  at each iteration  $k$  of the training process. A consensus mechanism is necessary to ensure  $\lim_{k \rightarrow \infty} \theta_1^{(k)} = \dots = \lim_{k \rightarrow \infty} \theta_m^{(k)}$ . To this end, we represent the update rule for each device  $i \in \mathcal{M}$  at each iteration  $k$  as in [15], [41]:

$$\theta_i^{(k+1)} = \theta_i^{(k)} + \sum_{j \in \mathcal{N}_i} p_{ij} \left( \theta_j^{(k)} - \theta_i^{(k)} \right) - \alpha^{(k)} g_i^{(k)}, \quad (14)$$

where  $p_{ij}$  is a mixing coefficient used for the model parameters of device pair  $(i, j)$  with a D2D link. Here, we employ the commonly used Metropolis-Hastings weights  $p_{ij} = \min\{1/(1 + |\mathcal{N}_i|), 1/(1 + |\mathcal{N}_j|)\}$  [42]. Furthermore,  $g_i^{(k)} = \nabla F_i(\theta_i^{(k)}, [\psi_j^{(k)}]_{j \in \mathcal{N}_i})$  is the style-based gradient of device  $i \in \mathcal{M}$  at iteration  $k$  obtained based on the local loss function, which will be elaborated in Sec. IV-A3. It has been well-established how the convergence speed of DFL in (14) decreases with the spectral radius  $\rho$  of the mixing matrix on the D2D graph  $\mathcal{G}$  [41], [43]; a core contribution of our work is expanding such results to style sharing in DG.

2) *Style Statistics:* Let  $X \in \mathbb{R}^{m \times B}$  be the concatenation of all local mini-batches of data from the devices, i.e.,  $X = [x_1 \dots x_m]^T$ . We denote the set of styles from all devices obtained using model parameters  $\theta$  and combined batch  $X$  for all devices as  $\Psi_\theta(X) = [\psi_\theta(x_1) \dots \psi_\theta(x_m)]^T$ . The style tensor that each device  $i \in \mathcal{M}$  calculates and shares with its neighbors is defined as  $\psi_\theta(x_i) = [\psi_{\theta,1}(x_i) \dots \psi_{\theta,L}(x_i)]^T$ , which is obtained for different CNN layers/blocks. Each individual style in this tensor consists of four style statistics at each layer/block  $\psi_{\theta,\ell}(x_i) = [\bar{\mu}_{\theta,\ell}(x_i) \quad \bar{\sigma}_{\theta,\ell}(x_i) \quad \Sigma_{\mu,\theta,\ell}^2(x_i) \quad \Sigma_{\sigma,\theta,\ell}^2(x_i)]^T$ :

$$\begin{aligned} \bar{\mu}_{\theta,\ell}(x_i)_c &= \frac{1}{B} \sum_{b=1}^B \mu(h_{\theta_\ell}(x_i))_{b,c}, \\ \bar{\sigma}_{\theta,\ell}(x_i)_c &= \frac{1}{B} \sum_{b=1}^B \sigma(h_{\theta_\ell}(x_i))_{b,c}, \end{aligned} \quad (15)$$

$$\Sigma_{\mu,\theta,\ell}^2(x_i)_c = \Sigma_\mu^2(h_{\theta_\ell}(x_i))_c, \quad \Sigma_{\sigma,\theta,\ell}^2(x_i)_c = \Sigma_\sigma^2(h_{\theta_\ell}(x_i))_c,$$

where functions  $\mu(\cdot)_{b,c}$  and  $\sigma(\cdot)_{b,c}$  are given in Eq. (2), and functions  $\Sigma_\mu^2(\cdot)_c$  and  $\Sigma_\sigma^2(\cdot)_c$  are given in Eq. (3).

Therefore, the dimensions of the style vectors will be  $\psi_{\theta_\ell}(x_i) \in \mathbb{R}^{4 \times C}$  for each layer,  $\psi_\theta(x_i) \in \mathbb{R}^{L \times 4 \times C}$  for each device and  $\Psi_\theta(X) \in \mathbb{R}^{m \times L \times 4 \times C}$  for the full network. Fig. 2 gives a detailed illustration of these style vectors and statistics.

*Remark 4.1:* (Communication overhead) The added communication overhead for sharing the style statistics  $\psi_\theta(x_i) \in \mathbb{R}^{L \times 4 \times C}$  is negligible relative to the model parameters  $\theta \in \mathbb{R}^n$ . Take the ResNet18 CNN model as an example, with around  $n = 11.69$  million parameters. The number of parameters in the full style statistics vector in STYLEDG will be 1792 (since there are four equidimensional style statistics at each layer, and they are calculated in the outputs of the first three convolutional blocks with channel numbers 64, 128 and 256,



$$F_i(\theta, \Psi) = \sum_{\pi \in \mathcal{P}(L)} \left( \prod_{\ell \in \pi} p_\ell \right) \mathbb{E}_{(x,y) \sim \mathbb{P}_{D_i}} \left[ \mathcal{L}(\tilde{h}_{\theta, \{\psi_{j_\ell}, \mathcal{R}_\ell\}_{\ell \in \pi}}(x), y) \right], \quad (20)$$

in which the expectation is taken over the set of random variables  $\mathcal{R}_\ell = \{\epsilon_{\mu, \ell}, \epsilon_{\sigma, \ell}, \lambda_\ell, \mathcal{I}_{s, \ell}, \mathcal{I}_{e, \ell}, \mathcal{I}_{m, \ell}\}$ , and the entries are sampled from the corresponding set of distributions  $\mathbb{P}_{\mathcal{R}} = \{\mathbb{P}_{\epsilon_\mu}, \mathbb{P}_{\epsilon_\sigma}, \mathbb{P}_\lambda, \mathcal{S}_{\mathcal{I}_s}, \mathcal{S}_{\mathcal{I}_e}, \mathcal{S}_B\}$ .  $\mathbb{P}_{D_i}$  denotes the probability distribution of source data in device  $i \in \mathcal{M}$ , and  $\mathcal{S}_{\mathcal{I}_s}$  and  $\mathcal{S}_{\mathcal{I}_e}$  are supersets of all unique permutations of the sets  $\mathcal{I}_s$  and  $\mathcal{I}_e$ , respectively. In turn,  $\mathcal{I}_s$  and  $\mathcal{I}_e$  are binary vectors of size  $B$ , with the number of 1s being equal to  $B_s$  and  $B_e$ , respectively. For a given layer  $\ell$ , each device  $i$  utilizes the received styles of a neighboring device  $j$  in the training process, i.e.,  $\psi_{j_\ell} = [\bar{\mu}_{j_\ell} \ \bar{\sigma}_{j_\ell} \ \Sigma_{\mu, j_\ell}^2 \ \Sigma_{\sigma, j_\ell}^2]^T$  as the  $j$ th element of  $\Psi$  in Eq. (20). In essence, STYLEDDG is applying a *style exploration* strategy to the outputs of the model's layer  $\ell$  with probability  $p_\ell$ , so that the overall model is modified as

$$\tilde{h}_{\theta, \{\psi_{j_\ell}, \mathcal{R}_\ell\}_{\ell \in \pi}}(x) = \left( \tilde{h}_{\theta_L, \psi_{j_L}, \mathcal{R}_L} \circ \dots \circ \tilde{h}_{\theta_1, \psi_{j_1}, \mathcal{R}_1} \right)(x), \quad (21)$$

in which  $\tilde{h}_{\theta_\ell, \psi_{j_\ell}, \mathcal{R}_\ell} = h_{\theta_\ell}$  if  $\ell \notin \pi$ . If  $\ell \in \pi$ , we define  $x_s = [x_k]_{k \in \{1, \dots, B\}; (\mathcal{I}_{s, \ell})_k = 1}^T$  as a subset of the mini-batch  $x$  based on the indices  $\mathcal{I}_{s, \ell}$  that we will shift to the styles of a neighboring device, and  $x_s^c = [x_k]_{k \in \{1, \dots, B\}; (\mathcal{I}_{s, \ell})_k = 0}^T$  as the ones which will not be shifted. Then the StyleExplore update that occurs at that layer can be expressed as

$$\tilde{h}_{\theta_\ell, \psi_{j_\ell}, \mathcal{R}_\ell}(x) = \text{StyleExplore} \left( \text{StyleShift}(h_{\theta_\ell}(x_s), h_{\theta_\ell}(x_s^c)), \lambda_\ell, \mathcal{I}_{m, \ell}, \mathcal{I}_{e, \ell}, \psi_{j_\ell}, \epsilon_{\mu, \ell}, \epsilon_{\sigma, \ell} \right), \quad (22)$$

where we first apply the StyleShift function on a given mini-batch  $x$  to randomly shift  $B_s$  of the points to new styles received from a neighbor, and then the StyleExplore layer takes the outputs of the StyleShift function to randomly extrapolate  $B_e$  of those styles outwards for style exploration.

## V. CONVERGENCE ANALYSIS

In this section, we characterize the convergence behavior of STYLEDDG. Papers such as [41], [43], [44] prove that in decentralized optimization of general non-convex models, convergence to stationary points can be guaranteed if the local loss functions are smooth, i.e., their gradients are Lipschitz continuous. To this end, we will discuss the conditions under which the smoothness of local loss functions in STYLEDDG given in Eq. (20) can be guaranteed as well. In other words, our goal is to prove that the upper bound  $\|\nabla F_i(\theta, \Psi) - \nabla F_i(\theta', \Psi')\| \leq \beta_i \|\theta - \theta'\|$  can be established for each device in STYLEDDG, where  $\beta_i \in \mathbb{R}^+$  is the smoothness coefficient.

Before we proceed, note that our main local loss function given in Eq. (20) essentially modifies the loss functions in a way that DG is achieved among the devices. We emphasize this to clarify what we mean by convergence in this context: whether the devices converge to the new optimal model with respect to the *modified* local loss functions.

### A. Assumptions

*Assumption 5.1: (Multivariate smoothness)* The local loss functions in Eq. (20) are smooth in their arguments, i.e.,

$$\|\nabla F_i(\theta, \Psi) - \nabla F_i(\theta', \Psi')\| \leq \beta_{\theta, i} \|\theta - \theta'\| + \beta_{\Psi, i} \|\Psi - \Psi'\|, \quad (23)$$

in which  $\beta_{\theta, i}, \beta_{\Psi, i} \in \mathbb{R}^+$  are positive scalars,  $\theta, \theta' \in \mathbb{R}^n$  are any two model parameters and  $\Psi, \Psi' \in \mathbb{R}^{|\mathcal{N}_i| \times L \times 4 \times C}$  are any two style vectors, for all  $i \in \mathcal{M}$ .

Assumption 5.1 is necessary to ensure the convergence of gradient-based methods, and it indicates that the local gradients do not change arbitrarily quickly [45]. The conventional smoothness assumption made in [43], [45] is of the form  $\|\nabla F_i(\theta) - \nabla F_i(\theta')\| \leq \beta_{\theta, i} \|\theta - \theta'\|$ . These works do not modify their CNN models with any style-based statistics, and the local loss functions are parameterized by  $\theta$  alone. Assumption 5.1 extends this to incorporate smoothness in terms of style vectors as well, i.e., the local loss functions do not change arbitrarily quickly with the style statistics.

*Remark 5.2: (Multivariate smoothness justification)* If we concatenate  $\theta$  and  $\Psi$  to form the vector  $\phi = [\theta^T, \Psi^T]^T$ , then the left-hand side of Eq. (23) can also be bounded as

$$\|\nabla F_i(\phi) - \nabla F_i(\phi')\| \leq \beta_{\phi, i} \|\phi - \phi'\|, \quad (24)$$

which is the standard smoothness assumption for a univariate function with  $\beta_{\phi, i} \in \mathbb{R}^+$ . Note that Eq. (24) is stricter than the multivariate smoothness assumption we use in Eq. (23) since we can obtain the former from the latter using triangle inequality.

*Assumption 5.3:* For each device  $i \in \mathcal{M}$  and layer  $\ell \in \{1, \dots, L\}$  of the CNN model  $\theta$ , the following holds for the outputs  $h_{\theta_\ell}(x_i)$  given an input  $x_i$  for device  $i$ :

- (Lipschitz continuity of layer outputs) We have  $\|h_{\theta_\ell}(x_i)_{b,c,h,w} - h_{\theta'_\ell}(x_i)_{b,c,h,w}\| \leq D_{i,\ell} \|\theta - \theta'\|$ , where  $\theta, \theta' \in \mathbb{R}^n$  are two arbitrary model parameter vectors and  $D_{i,\ell} \in \mathbb{R}^+$  is a positive scalar. Also, we define  $D_i = \max_\ell \{D_{i,\ell}\}$  and  $D = \max_i \{D_i\}$ .
- (Bounded layer outputs) For all  $\theta \in \mathbb{R}^n$ , there exists  $U_{i,\ell} \in \mathbb{R}^+$  such that  $\|h_{\theta_\ell}(x_i)_{b,c,h,w}\| \leq U_{i,\ell} < \infty$ . Also, we define  $U_i = \max_\ell \{U_{i,\ell}\}$  and  $U = \max_i \{U_i\}$ .

Assumption 5.3-(a) indicates that changes in the model parameters  $\theta$  do not lead to arbitrary large changes in the outputs of any layer. This is a safe assumption as the operations in CNNs (convolutional blocks, pooling layers, activation functions) behave this way. Assumption 5.3-(b) depends on the particular activation functions; for example, it holds for sigmoid, tanh and other bounded activations. With ReLU and other unbounded activations, for the purpose of our analysis, we only need this assumption to hold during the training phase.

### B. Main Results

We begin with Propositions 5.4 and 5.5, key results which provide guarantees for the smoothness of local loss functions in STYLEDDG. Subsequently, in Theorem 5.6, we use the propositions to show the convergence of STYLEDDG for general non-convex loss functions. In doing so, we ultimately

METHOD	ACCURACY FOR TARGET DOMAIN				
	ART	CARTOON	PHOTO	SKETCH	AVG
FEDBN	53.6 ± 0.9	48.9 ± 1.6	74.0 ± 1.9	53.4 ± 5.5	57.5
FEDBN + MixStyle	59.7 ± 1.5	55.5 ± 1.7	78.2 ± 1.0	55.7 ± 3.0	62.3
FEDBN + DSU	59.5 ± 1.0	55.9 ± 2.5	79.0 ± 1.4	59.7 ± 3.9	63.5
DSGD	67.7 ± 2.3	67.8 ± 1.1	91.1 ± 0.6	53.0 ± 9.9	69.9
DSGD + MixStyle	74.7 ± 1.0	71.1 ± 2.1	91.1 ± 0.5	58.9 ± 4.1	73.9
DSGD + DSU	76.6 ± 0.7	71.8 ± 1.0	91.7 ± 0.2	63.6 ± 3.0	75.9
STYLEDDG	<b>77.7 ± 0.4</b>	<b>73.0 ± 0.4</b>	<b>94.2 ± 0.3</b>	<b>66.2 ± 0.6</b>	<b>77.8</b>

TABLE I: Results on the PACS dataset, for a network of  $m = 3$  devices all connected to each other in a full mesh topology.

prove that the second term in our smoothness assumption given in Eq. (23), i.e.,  $\|\Psi - \Psi'\|$ , can also be bounded by  $\|\theta - \theta'\|$ .

*Proposition 5.4:* (Lipschitz continuity of style statistics) Let Assumption 5.3 hold. Then the style statistics from Eq. (15) are Lipschitz continuous at each layer/block  $\ell = \{1, \dots, L\}$  of the CNN  $\theta$  for all devices  $i \in \mathcal{M}$ , and for all channels  $c \in \{1, \dots, C\}$ . Specifically:

- (a)  $\|\bar{\mu}_{\theta,\ell}(x_i)_c - \bar{\mu}_{\theta',\ell}(x_i)_c\| \leq D_{i,\ell} \|\theta - \theta'\|$
- (b)  $\|\bar{\sigma}_{\theta,\ell}(x_i)_c - \bar{\sigma}_{\theta',\ell}(x_i)_c\| \leq \frac{4U_i D_{i,\ell}}{\sqrt{\eta}} \|\theta - \theta'\|$
- (c)  $\|\Sigma_{\mu,\theta,\ell}^2(x_i)_c - \Sigma_{\mu,\theta',\ell}^2(x_i)_c\| \leq 4U_i D_{i,\ell} \|\theta - \theta'\|$
- (d)  $\|\Sigma_{\sigma,\theta,\ell}^2(x_i)_c - \Sigma_{\sigma,\theta',\ell}^2(x_i)_c\| \leq 4U_i D_{i,\ell} (1 + \frac{2\sqrt{2}U_i}{\sqrt{\eta}}) \|\theta - \theta'\|$

*Sketch of Proof.*<sup>1</sup> For each of the style statistics, we start the derivation of the upper bound using their corresponding definitions in Eq. (15). Part (a) requires only the Lipschitzness of CNN outputs  $h_\theta(x)$  (Assumption 5.3-(a)). Part (b) requires us to establish the Lipschitzness of  $h_\theta^2(x)$  (where the boundedness of CNN outputs defined in Assumption 5.3-(b) is used), and then use the lower bound for  $\sigma_\theta(x)$  enforced by the numerical stability value  $\eta$  to conclude the proof. A crucial piece of part (b)'s proof is to derive the bounds in such a way that the stability parameter  $\eta$  can be used to obtain the bounds, which has not been investigated in earlier works [28]. Finally, parts (c) and (d) use parts (a) and (b) to obtain upper bounds for their variances, respectively.

Proposition 5.4 shows that if the style statistics given in Eq. (15) are calculated via the model  $\theta$  on any data batch  $X$ , the resulting statistics will be Lipschitz with respect to  $\theta$ . With this result in hand, we can now prove the smoothness of local and global loss functions given in Eqs. (20) and (19).

*Proposition 5.5:* (Univariate smoothness) Let Assumptions 5.1 and 5.3 hold. Then for any  $\theta, \theta' \in \mathbb{R}^n$ , it holds that for any given combined batch  $X$  across devices, the local loss function of each device  $i \in \mathcal{M}$  is smooth, i.e.,

$$\|\nabla F_i(\theta, \Psi_{\theta,i}(X)) - \nabla F_i(\theta', \Psi_{\theta',i}(X))\| \leq \beta_i \|\theta - \theta'\|,$$

where  $\beta_i = \beta_{\theta,i} + mL(1 + 4U(\frac{1}{\sqrt{\eta}} + 2 + \frac{2\sqrt{2}U}{\sqrt{\eta}}))D\beta_{\Psi,i}$ ,  $\beta_{\theta,i}$  and  $\beta_{\Psi,i}$  are provided in Assumption 5.1,  $m$  is the total number of devices,  $L$  is the number of layers which STYLEDDG is applied to,  $U$  and  $D$  are the bounds from Assumption 5.3, and  $\eta > 0$  is the small numerical stability constant.

*Sketch of Proof.* With the Lipschitzness of all four individual style statistics of each device and layer/block

established in Proposition 5.4, we first establish the Lipschitz continuity of their concatenation  $\psi_{\theta,\ell}(x_i) = [\bar{\mu}_{\theta,\ell}(x_i) \ \bar{\sigma}_{\theta,\ell}(x_i) \ \Sigma_{\mu,\theta,\ell}^2(x_i) \ \Sigma_{\sigma,\theta,\ell}^2(x_i)]^T$ . Next, we focus on the Lipschitzness of style statistics across all the layers of the CNN for a given client  $i \in \mathcal{M}$ , i.e.,  $\psi_\theta(x_i) = [\psi_{\theta,1}(x_i) \ \dots \ \psi_{\theta,L}(x_i)]^T$ . This helps us to ultimately prove the Lipschitzness of full style statistics matrix  $\Psi_\theta(X) = [\psi_\theta(x_1) \ \dots \ \psi_\theta(x_m)]^T$ .

In Proposition 5.5, note that smaller  $U = \max_{i,\ell} U_{i,\ell}$ , smaller  $D = \max_{i,\ell} D_{i,\ell}$ , and larger  $\eta$  each result in a smaller smoothness parameter  $\beta$ . This corresponds to a faster convergence during training.

*Theorem 5.6:* Let Assumptions 5.1 and 5.3 hold, and a constant learning rate  $\alpha^{(k)} = \alpha^{(0)}/\sqrt{K+1}$  be employed, where  $K$  is the maximum number of iterations that STYLEDDG will run. Then, for general non-convex loss model, we have

$$\frac{\sum_{k=0}^K \|\nabla F(\bar{\theta}^{(k)})\|^2}{K+1} \leq \frac{F(\bar{\theta}^{(0)}) - F^*}{\mathcal{O}(\sqrt{K+1})} + \frac{1+\rho}{(1-\rho)^2} \frac{\beta^2}{\mathcal{O}(K+1)} + \frac{\beta/(2m)}{\mathcal{O}(\sqrt{K+1})}, \quad (25)$$

where  $\beta = (1/m) \sum_{i=1}^m \beta_i$ ,  $F^* = \min_{\theta \in \mathbb{R}^n} \{F(\theta)\}$ ,  $m$  denotes the number of devices,  $\bar{\theta}^{(k)} = (1/m) \sum_{i=1}^m \theta_i^{(k)}$  is the average model among all devices at iteration  $k$ ,  $\rho$  is the spectral radius of the connected network graph  $\mathcal{G}$ , and  $\beta$  is the smoothness parameter given by Proposition 5.5.

*Sketch of Proof.* With the univariate smoothness of local loss functions established in Proposition 5.5, we can build upon established theoretical results in decentralized optimization to provide convergence guarantees. The proof can follow steps similar to e.g., Theorem 4.12 in [41] or Lemma 16 in [43].

Theorem 5.6 shows that STYLEDDG reaches a stationary point for general non-convex models at a rate of  $\mathcal{O}(1/\sqrt{K})$ . To be specific, after running STYLEDDG for  $K$  iterations with a learning rate proportional to  $1/\sqrt{K+1}$ , the running average ( $\frac{1}{K+1} \sum_{k=0}^K (\cdot)$ ) of global gradient norm expectations ( $\mathbb{E}[\|\nabla F(\cdot)\|]$ ), evaluated at the average model  $\bar{\theta}^{(k)}$ , is proportional to  $1/\sqrt{K+1}$ . This bound becomes arbitrarily small as the training progresses, i.e., by increasing  $K$ . Further, in Theorem 5.6, learning model-related parameters of Assumptions 5.1 and 5.3, i.e., multivariate smoothness parameters  $\beta_{\theta,i}$  and  $\beta_{\Psi,i}$ , Lipschitz constant  $D_{i,\ell}$  and upper bound  $U_{i,\ell}$ , are all captured in the univariate smoothness parameter  $\beta$  derived in Proposition 5.5. We see in Eq. (25) that a lower smoothness value  $\beta$ , as well as a better-connected D2D graph (i.e., smaller spectral radius  $\rho$ ), results in a smaller upper bound in Eq. (25), accelerating the convergence speed accordingly.

## VI. NUMERICAL EXPERIMENTS

### A. Setup

**Datasets and Model.** Our experiments are based on two widely-used benchmark datasets for DG: (i) PACS [40] which consists of 4 domains (art painting (A), cartoon (C), photo (P), and sketch (S)) and contains 7 classes of images (dog,

<sup>1</sup>Due to space limitations, we are only able to provide a sketch of each proof. In the camera-ready, we will provide a technical report with full proofs.

METHOD	ACCURACY FOR TARGET DOMAIN				
	ART	CARTOON	PHOTO	SKETCH	AVG
FEDBN	40.2 ± 0.9	35.5 ± 0.3	52.7 ± 1.4	34.0 ± 0.7	40.6
FEDBN + MixStyle	42.2 ± 1.0	39.1 ± 0.3	53.6 ± 1.4	38.6 ± 0.2	43.4
FEDBN + DSU	42.6 ± 0.8	40.8 ± 0.8	56.8 ± 2.4	39.3 ± 0.6	44.9
DSGD	58.8 ± 1.1	52.5 ± 2.1	78.0 ± 2.0	36.7 ± 5.2	56.5
DSGD + MixStyle	<b>60.8 ± 1.4</b>	55.6 ± 1.9	73.3 ± 0.9	39.9 ± 4.9	57.4
DSGD + DSU	56.8 ± 1.2	54.1 ± 1.7	78.2 ± 3.4	35.5 ± 4.8	56.1
STYLEDDG	60.6 ± 1.6	<b>56.3 ± 2.0</b>	<b>81.5 ± 4.0</b>	<b>42.3 ± 4.5</b>	<b>60.2</b>

TABLE II: Results on the PACS dataset, for a network of  $m = 9$  devices over a random geometric graph with radius  $r = 0.8$ .

METHOD	ACCURACY FOR TARGET DOMAIN				
	CALTECH	LABELME	PASCAL	SUN	AVG
FEDBN	95.5 ± 0.8	56.6 ± 0.5	65.1 ± 0.7	66.1 ± 0.6	70.8
FEDBN + MixStyle	96.7 ± 0.5	57.2 ± 0.5	65.8 ± 0.4	66.9 ± 0.7	71.6
FEDBN + DSU	97.4 ± 0.2	56.5 ± 0.3	66.4 ± 0.3	67.1 ± 0.4	71.9
DSGD	96.3 ± 0.8	56.0 ± 0.5	67.9 ± 0.6	68.5 ± 1.0	72.2
DSGD + MixStyle	98.0 ± 0.6	56.9 ± 0.7	67.7 ± 1.8	<b>70.1 ± 1.4</b>	73.2
DSGD + DSU	98.4 ± 0.3	56.1 ± 0.3	68.6 ± 0.6	69.9 ± 1.4	73.2
STYLEDDG	<b>98.6 ± 0.8</b>	<b>58.1 ± 1.2</b>	<b>69.4 ± 0.1</b>	69.4 ± 1.4	<b>73.9</b>

TABLE III: Results on the VLCS dataset, for a network of  $m = 3$  devices all connected to each other.

elephant, giraffe, guitar, horse, house, and person); and (ii) VLCS [46] with 4 domains (Caltech101, LabelMe, PASCAL VOC2007, and SUN09) and 5 categories of images (bird, car, chair, dog, and person). For both datasets, we use 3 domains as the source domains and reserve the remaining one as the target domain (for evaluating the test performance). By default, we conduct our experiments using the ResNet18 model [39].

**Baselines.** Since our work is the first to propose a fully decentralized DG algorithm, we select some centralized and federated DG algorithms and implement a decentralized realization of them for comparison. Specifically, we compare STYLEDDG against DSGD [43], FedBN [32], MixStyle [28] and DSU [29]. For the well-known style-based centralized DG methods, MixStyle and DSU, we incorporate these algorithms into the local update process at each client.

**Setting.** Our experiments are done under two sets of networks: (i)  $m = 3$  devices, and (ii)  $m = 9$  devices, connected together over a random geometric graph [47]. The choice of 3-9 edge devices aligns with the conventions of experiments found in existing FDG literature [32], [48], [49], thus providing fair comparisons with the baselines. Our implementation of STYLEDDG is based on the DASSL library developed in [6], [50]. We adopt a constant learning rate  $\alpha = 0.001$  with a cosine scheduler, and use the batch size of 64. We distribute the data among the edge devices in a domain-heterogeneous way, where each device receives samples only from a single domain. We measure the test accuracy of each algorithm after 50 epochs of training. We conduct the experiments based on a cluster of four NVIDIA A100 GPUs with 40GB memory. We run the experiments five times in each setup, and present the mean and standard deviation.

METHOD	ACCURACY FOR TARGET DOMAIN				
	ART	CARTOON	PHOTO	SKETCH	AVG
FEDBN	61.5 ± 0.6	51.8 ± 1.2	85.9 ± 1.1	59.5 ± 1.1	64.7
FEDBN + MixStyle	63.7 ± 0.8	60.1 ± 0.8	86.8 ± 0.5	65.0 ± 2.1	68.9
FEDBN + DSU	69.2 ± 1.7	59.1 ± 0.9	88.7 ± 1.1	69.1 ± 1.2	71.5
DSGD	78.9 ± 0.4	75.2 ± 0.3	94.5 ± 0.3	65.8 ± 1.6	78.6
DSGD + MixStyle	81.8 ± 0.7	<b>79.5 ± 0.6</b>	94.7 ± 0.3	70.5 ± 0.9	81.6
DSGD + DSU	84.1 ± 0.5	77.2 ± 0.4	95.5 ± 0.0	74.4 ± 1.2	82.8
STYLEDDG	<b>87.5 ± 0.4</b>	78.9 ± 0.3	<b>97.4 ± 0.1</b>	<b>75.6 ± 1.0</b>	<b>84.9</b>

TABLE IV: Results on the PACS dataset, for a network of  $m = 3$  devices all connected to each other using ResNet50.

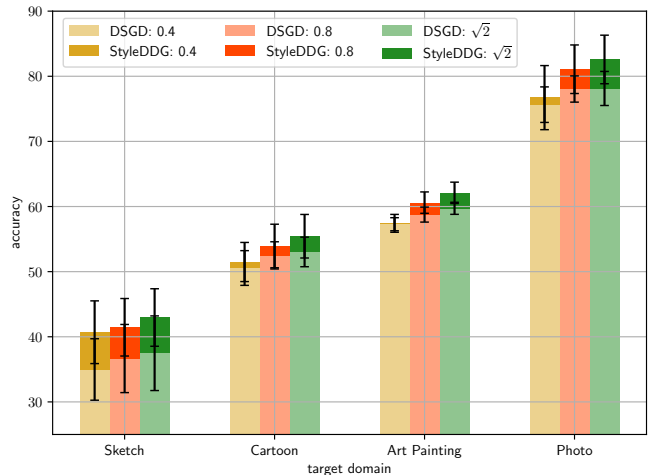


Fig. 3: Results on the PACS dataset for different target domains, for a network of  $m = 9$  clients over a random geometric graph with varying radius  $r = 0.4, 0.8, \sqrt{2}$ .

## B. Results and Discussion

**PACS.** Table I shows the result with PACS dataset with  $m = 3$  clients. We make the following observations. First, existing style-based centralized DG methods, i.e., MixStyle and DSU, enhance the performance of both FedBN and DSGD by exposing models to a diversity of styles. However, applying these approaches does not allow the model to sufficiently explore diverse styles, as each device has access to only a limited set of styles or domains. We observe that STYLEDDG addresses this limitation through style sharing and exploration in decentralized settings, resulting in a significant improvement in generalization capability.

Table II extends our results to  $m = 9$  devices connected via a random geometric graph with radius  $r = 0.8$ . We see that the performance gain of STYLEDDG over the baselines becomes more pronounced, highlighting its advantage in larger networks with less connectivity among devices.

**VLCS.** In Table III, we evaluate performance on the VLCS dataset. Although the gains are smaller than those observed on PACS – due to the relatively smaller style gap between domains in VLCS [13] – STYLEDDG still outperforms on all but one domain.

**ResNet50.** In Table IV, we explore the DG performance of our algorithm using a larger model, i.e., ResNet50 [39]. Our results show that STYLEDDG outperforms all baselines in all but one domain, and is superior to them on average. Also, compared to ResNet18 results from Table I, we see  $\sim 7\%$

increase in accuracy of all DG algorithms, which shows that larger models lead to higher-quality style statistics for DG.

**Graph Connectivity.** In Fig. 3, we vary radius of the random geometric graph in a network of  $m = 9$  devices and compare the performance of STYLEDG with DSDG for different connectivity levels of the network. We observe that our methodology maintains its superiority across different connectivity levels. Furthermore, the advantage of our method increases with higher graph connectivity, showing that it can better utilize the underlying network topology to achieve DG. In other words, the strength of style sharing in our method becomes more significant if each device is connected to more neighbors, as it can be exposed to a larger set of styles.

## VII. CONCLUSION

We proposed STYLEDG, to our knowledge the first decentralized federated domain generalization algorithm. STYLEDG enables edge devices in a decentralized network to train domain-invariant models. We achieved this by forming consensus-based model aggregation and style sharing, and developing a style exploration strategy to expose each device to the new style domains from their neighbors. Further, we provided a novel analytical foundation of well-known domain generalization methods and extended it to our methodology, enabling us to conduct the first convergence analysis among all style-based domain generalization algorithms. Our experiments demonstrated the effectiveness of STYLEDG compared to other domain generalization baselines in terms of model accuracy on unseen target domains.

## REFERENCES

- [1] P. Kairouz, H. B. McMahan, B. Avent, A. Bellet, M. Bennis, A. N. Bhagoji, K. Bonawitz, Z. Charles, G. Cormode, R. Cummings *et al.*, “Advances and open problems in federated learning,” *Foundations and trends® in machine learning*, vol. 14, no. 1–2, pp. 1–210, 2021.
- [2] B. McMahan, E. Moore, D. Ramage, S. Hampson, and B. A. y Arcas, “Communication-efficient learning of deep networks from decentralized data,” in *AISTATS*. PMLR, 2017, pp. 1273–1282.
- [3] C. G. Brinton, M. Chiang, K. T. Kim, D. J. Love, M. Beesley, M. Repeta, J. Roese, P. Beming, E. Ekudden, C. Li *et al.*, “Key focus areas and enabling technologies for 6g,” *IEEE Communications Magazine*, vol. 63, no. 3, pp. 84–91, 2025.
- [4] L. Yuan, Z. Wang, L. Sun, P. S. Yu, and C. G. Brinton, “Decentralized federated learning: A survey and perspective,” *IEEE Internet of Things Journal*, vol. 11, no. 21, pp. 34 617–34 638, 2024.
- [5] A. Nedic and A. Ozdaglar, “Distributed subgradient methods for multi-agent optimization,” *IEEE Transactions on Automatic Control*, vol. 54, no. 1, pp. 48–61, 2009.
- [6] K. Zhou, Z. Liu, Y. Qiao, T. Xiang, and C. C. Loy, “Domain generalization: A survey,” *IEEE Transactions on Pattern Analysis and Machine Intelligence*, vol. 45, no. 4, pp. 4396–4415, 2022.
- [7] S. Ben-David, J. Blitzer, K. Crammer, A. Kulesza, F. Pereira, and J. W. Vaughan, “A theory of learning from different domains,” *Machine learning*, vol. 79, pp. 151–175, 2010.
- [8] A. Filos, P. Tigkas, R. McAllister, N. Rhinehart, S. Levine, and Y. Gal, “Can autonomous vehicles identify, recover from, and adapt to distribution shifts?” in *ICLR*. PMLR, 2020, pp. 3145–3153.
- [9] J. Wang, C. Lan, C. Liu, Y. Ouyang, T. Qin, W. Lu, Y. Chen, W. Zeng, and S. Y. Philip, “Generalizing to unseen domains: A survey on domain generalization,” *IEEE transactions on knowledge and data engineering*, vol. 35, no. 8, pp. 8052–8072, 2022.
- [10] R. Bai, S. Bagchi, and D. I. Inouye, “Benchmarking algorithms for federated domain generalization,” in *ICLR*, 2024.
- [11] Y. Li, X. Wang, R. Zeng, P. K. Donta, I. Murturi, M. Huang, and S. Dustdar, “Federated domain generalization: A survey,” *arXiv preprint arXiv:2306.01334*, 2023.
- [12] S. Wang, S. Hosseinalipour, and C. G. Brinton, “Multi-source to multi-target decentralized federated domain adaptation,” *IEEE Transactions on Cognitive Communications and Networking*, vol. 10, no. 3, pp. 1011–1025, 2024.
- [13] J. Park, D.-J. Han, J. Kim, S. Wang, C. Brinton, and J. Moon, “Stablefdg: style and attention based learning for federated domain generalization,” *NeurIPS*, vol. 36, 2024.
- [14] R. Parasnis, S. Hosseinalipour, Y.-W. Chu, M. Chiang, and C. G. Brinton, “Connectivity-aware semi-decentralized federated learning over time-varying d2d networks,” in *ACM MobiHoc*, 2023, pp. 31–40.
- [15] E. Chen, S. Wang, and C. G. Brinton, “Taming subnet-drift in d2d-enabled fog learning: A hierarchical gradient tracking approach,” in *IEEE INFOCOM*, 2024, pp. 2438–2447.
- [16] S. Hosseinalipour, C. G. Brinton, V. Aggarwal, H. Dai, and M. Chiang, “From federated to fog learning: Distributed machine learning over heterogeneous wireless networks,” *IEEE Communications Magazine*, vol. 58, no. 12, pp. 41–47, 2020.
- [17] A. Nedić, A. Olshevsky, and M. G. Rabbat, “Network topology and communication-computation tradeoffs in decentralized optimization,” *Proceedings of the IEEE*, vol. 106, no. 5, pp. 953–976, 2018.
- [18] W. Liu, L. Chen, and W. Wang, “General decentralized federated learning for communication-computation tradeoff,” in *IEEE INFOCOM WKSHPs*, 2022, pp. 1–6.
- [19] X. Zhang, M. Fang, Z. Liu, H. Yang, J. Liu, and Z. Zhu, “Net-fleet: Achieving linear convergence speedup for fully decentralized federated learning with heterogeneous data,” in *ACM MobiHoc*, 2022, pp. 71–80.
- [20] J. Zhang, L. Chen, X. Chen, and G. Wei, “A novel hierarchically decentralized federated learning framework in 6g wireless networks,” in *INFOCOM WKSHPs*. IEEE, 2023, pp. 1–6.
- [21] Y. Huang, T. Sun, and T. He, “Overlay-based decentralized federated learning in bandwidth-limited networks,” in *ACM MobiHoc*, 2024, pp. 121–130.
- [22] D. Li, Y. Yang, Y.-Z. Song, and T. Hospedales, “Learning to generalize: Meta-learning for domain generalization,” in *AAAI*, vol. 32, no. 1, 2018.
- [23] Y. Balaji, S. Sankaranarayanan, and R. Chellappa, “Metareg: Towards domain generalization using meta-regularization,” *NeurIPS*, vol. 31, 2018.
- [24] F. M. Carlucci, A. D’Innocente, S. Bucci, B. Caputo, and T. Tommasi, “Domain generalization by solving jigsaw puzzles,” in *IEEE CVPR*, 2019, pp. 2229–2238.
- [25] Z. Huang, H. Wang, E. P. Xing, and D. Huang, “Self-challenging improves cross-domain generalization,” in *ECCV*. Springer, 2020, pp. 124–140.
- [26] M. Ghifary, W. B. Kleijn, M. Zhang, and D. Balduzzi, “Domain generalization for object recognition with multi-task autoencoders,” in *ICCV*, 2015, pp. 2551–2559.
- [27] H. Li, S. J. Pan, S. Wang, and A. C. Kot, “Domain generalization with adversarial feature learning,” in *IEEE CVPR*, 2018, pp. 5400–5409.
- [28] K. Zhou, Y. Yang, Y. Qiao, and T. Xiang, “Domain generalization with mixstyle,” *ICLR*, 2021.
- [29] X. Li, Y. Dai, Y. Ge, J. Liu, Y. Shan, and L.-Y. Duan, “Uncertainty modeling for out-of-distribution generalization,” *ICLR*, 2022.
- [30] X. Huang and S. Belongie, “Arbitrary style transfer in real-time with adaptive instance normalization,” in *ICCV*, 2017, pp. 1501–1510.
- [31] T. Li, A. K. Sahu, A. Talwalkar, and V. Smith, “Federated learning: Challenges, methods, and future directions,” *IEEE signal processing magazine*, vol. 37, no. 3, pp. 50–60, 2020.
- [32] X. Li, M. JIANG, X. Zhang, M. Kamp, and Q. Dou, “Fedbn: Federated learning on non-iid features via local batch normalization,” in *ICLR*, 2021.
- [33] Q. Liu, C. Chen, J. Qin, Q. Dou, and P.-A. Heng, “Feddg: Federated domain generalization on medical image segmentation via episodic learning in continuous frequency space,” in *Proceedings of the IEEE/CVF conference on computer vision and pattern recognition*, 2021, pp. 1013–1023.
- [34] G. Wu and S. Gong, “Collaborative optimization and aggregation for decentralized domain generalization and adaptation,” in *ICCV*, 2021, pp. 6484–6493.
- [35] J. Chen, M. Jiang, Q. Dou, and Q. Chen, “Federated domain generalization for image recognition via cross-client style transfer,” in *IEEE/CVF WACV*, 2023, pp. 361–370.

- [36] R. Zhang, Q. Xu, J. Yao, Y. Zhang, Q. Tian, and Y. Wang, "Federated domain generalization with generalization adjustment," in *ICCV*, 2023, pp. 3954–3963.
- [37] J. Kang, S. Lee, N. Kim, and S. Kwak, "Style neophile: Constantly seeking novel styles for domain generalization," in *Proceedings of the IEEE/CVF Conference on Computer Vision and Pattern Recognition*, 2022, pp. 7130–7140.
- [38] J. Park, D.-J. Han, S. Kim, and J. Moon, "Test-time style shifting: Handling arbitrary styles in domain generalization," in *ICLR*. PMLR, 2023, pp. 27 114–27 131.
- [39] K. He, X. Zhang, S. Ren, and J. Sun, "Deep residual learning for image recognition," in *IEEE CVPR*, 2016, pp. 770–778.
- [40] D. Li, Y. Yang, Y.-Z. Song, and T. M. Hospedales, "Deeper, broader and artier domain generalization," in *ICCV*, 2017, pp. 5542–5550.
- [41] S. Zehetabi, D.-J. Han, R. Parasnis, S. Hosseinalipour, and C. G. Brinton, "Decentralized sporadic federated learning: A unified algorithmic framework with convergence guarantees," *ICLR*, 2025.
- [42] L. Xiao and S. Boyd, "Fast linear iterations for distributed averaging," *Systems & Control Letters*, vol. 53, no. 1, pp. 65–78, 2004.
- [43] A. Koloskova, N. Loizou, S. Boreiri, M. Jaggi, and S. Stich, "A unified theory of decentralized sgd with changing topology and local updates," in *ICML*. PMLR, 2020, pp. 5381–5393.
- [44] R. Xin, U. A. Khan, and S. Kar, "An improved convergence analysis for decentralized online stochastic non-convex optimization," *IEEE Transactions on Signal Processing*, vol. 69, pp. 1842–1858, 2021.
- [45] L. Bottou, F. E. Curtis, and J. Nocedal, "Optimization methods for large-scale machine learning," *SIAM review*, vol. 60, no. 2, pp. 223–311, 2018.
- [46] A. Torralba and A. A. Efros, "Unbiased look at dataset bias," in *IEEE CVPR*. IEEE, 2011, pp. 1521–1528.
- [47] M. Penrose, *Random geometric graphs*. OUP Oxford, 2003, vol. 5.
- [48] L. Zhang, X. Lei, Y. Shi, H. Huang, and C. Chen, "Federated learning with domain generalization," *arXiv preprint arXiv:2111.10487*, 2021.
- [49] A. T. Nguyen, P. Torr, and S. N. Lim, "Fedrs: A simple and effective domain generalization method for federated learning," in *NeurIPS*, vol. 35, 2022, pp. 38 831–38 843.
- [50] K. Zhou, Y. Yang, Y. Qiao, and T. Xiang, "Domain adaptive ensemble learning," *IEEE Transactions on Image Processing*, vol. 30, pp. 8008–8018, 2021.

## APPENDIX

*Lemma A.1:* (Bounded  $\mu$  and  $\sigma$  style statistics) Let Assumption 5.3-(b) hold. Then for all devices  $i \in \mathcal{M}$  and all layers/blocks  $\ell \in \{1, \dots, L\}$  of the CNN  $\theta$  it holds that

- (a)  $\|\mu(h_{\theta_\ell}(x_i))_{b,c}\| \leq U_{i,\ell}$ ,
- (b)  $\|\sigma(h_{\theta_\ell}(x_i))_{b,c}\| \leq \sqrt{2}U_{i,\ell} + \sqrt{\eta}$ ,
- (c)  $\|\bar{\mu}_{\theta,\ell}(x_i)_c\| \leq U_{i,\ell}$ .
- (d)  $\|\bar{\sigma}_{\theta,\ell}(x_i)_c\| \leq \sqrt{2}U_{i,\ell} + \sqrt{\eta}$ ,

where  $U_{i,\ell}$  is provided in Assumption 5.3.

Note that Lemma A.1-(b) together with the definition given in Eq. (2) establish the bounds

$$\sqrt{\eta} \leq \|\sigma(h_{\theta_\ell}(x_i))_{b,c}\| \leq U_{i,\ell}. \quad (26)$$

Equipped with Lemma A.1, we move on to presenting the next key result which establishes the Lipschitz continuity of all style statistics used in STYLEDG.

*Proof A.2:* (a) Using the definition of  $\mu(\cdot)_{b,c}$  from Eq. (2), we have

$$\begin{aligned} \|\mu(h_{\theta_\ell}(x_i))_{b,c}\| &= \left\| \frac{1}{HW} \sum_{h=1}^H \sum_{w=1}^W h_{\theta_\ell}(x_i)_{b,c,h,w} \right\| \\ &\leq \frac{1}{HW} \sum_{h=1}^H \sum_{w=1}^W \|h_{\theta_\ell}(x_i)_{b,c,h,w}\| \leq \frac{1}{HW} \sum_{h=1}^H \sum_{w=1}^W U_{i,\ell} \\ &= U_{i,\ell}, \end{aligned} \quad (27)$$

in which we used the triangle inequality.

*Proof A.3:* (b) We first find an upper bound for  $\|\sigma^2(h_{\theta_\ell}(x_i))_{b,c}\|$ , and then take the square root of those to conclude the proof. Using the definition of  $\sigma^2(\cdot)_{b,c}$  from Eq. (2), we first rewrite its definition as

$$\begin{aligned} \sigma^2(h_{\theta_\ell}(x_i))_{b,c} &= \frac{1}{HW} \sum_{h=1}^H \sum_{w=1}^W (h_{\theta_\ell}(x_i)_{b,c,h,w} - \mu(h_{\theta_\ell}(x_i))_{b,c})^2 + \eta \\ &= \frac{1}{HW} \sum_{h=1}^H \sum_{w=1}^W h_{\theta_\ell}(x_i)_{b,c,h,w}^2 - \mu(h_{\theta_\ell}(x_i))_{b,c}^2 + \eta. \end{aligned} \quad (28)$$

Using this definition, we can write the following

$$\begin{aligned} \|\sigma^2(h_{\theta_\ell}(x_i))_{b,c}\| &= \left\| \frac{1}{HW} \sum_{h=1}^H \sum_{w=1}^W h_{\theta_\ell}(x_i)_{b,c,h,w}^2 - \mu(h_{\theta_\ell}(x_i))_{b,c}^2 + \eta \right\| \\ &\leq \frac{1}{HW} \sum_{h=1}^H \sum_{w=1}^W \|h_{\theta_\ell}(x_i)_{b,c,h,w}\|^2 + \|\mu(h_{\theta_\ell}(x_i))_{b,c}\|^2 + \eta \\ &\leq \frac{1}{HW} \sum_{h=1}^H \sum_{w=1}^W U_{i,\ell}^2 + U_{i,\ell}^2 + \eta = 2U_{i,\ell}^2 + \eta, \end{aligned} \quad (29)$$

in which we used the triangle inequality, and then invoked the results of Assumption 5.3-(b) and Lemma A.1-(a). Taking the square root of the above inequality, we get

$$\|\sigma(h_{\theta_\ell}(x_i))_{b,c}\| \leq \sqrt{2U_{i,\ell}^2 + \eta} \leq \sqrt{2}U_{i,\ell} + \sqrt{\eta}. \quad (30)$$

*Proof A.4:* (c) Using the definition of  $\bar{\mu}_{\theta,\ell}(x_i)_c$  from Eq. (15), we have

$$\begin{aligned} \|\bar{\mu}_{\theta,\ell}(x_i)_c\| &= \left\| \frac{1}{B} \sum_{b=1}^B \mu(h_{\theta_\ell}(x_i))_{b,c} \right\| \\ &\leq \frac{1}{B} \sum_{b=1}^B \|\mu(h_{\theta_\ell}(x_i))_{b,c}\| \leq \frac{1}{B} \sum_{b=1}^B U_{i,\ell} = U_{i,\ell}, \end{aligned} \quad (31)$$

in which we used the triangle inequality and then invoked the result of Lemma A.1-(a).

*Proof A.5:* (d) Using the definition of  $\bar{\sigma}_{\theta,\ell}(x_i)_c$  from Eq. (15), we have

$$\begin{aligned} \|\bar{\sigma}_{\theta,\ell}(x_i)_c\| &= \left\| \frac{1}{B} \sum_{b=1}^B \sigma(h_{\theta_\ell}(x_i))_{b,c} \right\| \\ &\leq \frac{1}{B} \sum_{b=1}^B \|\sigma(h_{\theta_\ell}(x_i))_{b,c}\| \leq \frac{1}{B} \sum_{b=1}^B (\sqrt{2}U_{i,\ell} + \sqrt{\eta}) \\ &= \sqrt{2}U_{i,\ell} + \sqrt{\eta}, \end{aligned} \quad (32)$$

in which we used the triangle inequality and then invoked the result of Lemma A.1-(b).

*Proof A.6:* (a) Using the definition  $\bar{\mu}_{\theta,\ell}(x_i)_c = \frac{1}{B} \sum_{b=1}^B \mu(h_{\theta_\ell}(x_i))_{b,c}$  given in Eq. (15), we have that

$$\begin{aligned} & \|\bar{\mu}_{\theta,\ell}(x_i)_c - \bar{\mu}_{\theta',\ell}(x_i)_c\| \\ & \leq \left\| \frac{1}{B} \sum_{b=1}^B (\mu(h_{\theta_\ell}(x_i))_{b,c} - \mu(h_{\theta'_\ell}(x_i))_{b,c}) \right\| \\ & \leq \frac{1}{B} \sum_{b=1}^B \|\mu(h_{\theta_\ell}(x_i))_{b,c} - \mu(h_{\theta'_\ell}(x_i))_{b,c}\|, \end{aligned} \quad (33)$$

in which we used the triangle inequality. Therefore, we must establish Lipschitz continuity of  $\mu(h_{\theta_\ell}(x_i))_{b,c}$ . Using the definition of the function  $\mu(\cdot)_{b,c}$  given in Eq. (2), we have that

$$\begin{aligned} & \|\mu(h_{\theta_\ell}(x_i))_{b,c} - \mu(h_{\theta'_\ell}(x_i))_{b,c}\| \\ & \leq \left\| \frac{1}{HW} \sum_{h=1}^H \sum_{w=1}^W (h_{\theta_\ell}(x_i)_{b,c,h,w} - h_{\theta'_\ell}(x_i)_{b,c,h,w}) \right\| \\ & \leq \frac{1}{HW} \sum_{h=1}^H \sum_{w=1}^W \|h_{\theta_\ell}(x_i)_{b,c,h,w} - h_{\theta'_\ell}(x_i)_{b,c,h,w}\| \\ & \leq \frac{1}{HW} \sum_{h=1}^H \sum_{w=1}^W D_{i,\ell} \|\theta - \theta'\| = D_{i,\ell} \|\theta - \theta'\|, \end{aligned} \quad (34)$$

where we used the triangle inequality first, then invoked Assumption 5.3-(a). Plugging the result of Eq. (34) back in Eq. (33), we obtain

$$\|\bar{\mu}_{\theta,\ell}(x_i)_c - \bar{\mu}_{\theta',\ell}(x_i)_c\| \leq \frac{1}{B} \sum_{b=1}^B D_{i,\ell} \|\theta - \theta'\| = D_{i,\ell} \|\theta - \theta'\|. \quad (35)$$

*Proof A.7:* (b) Using the definition  $\bar{\sigma}_{\theta,\ell}(x_i)_c = \frac{1}{B} \sum_{b=1}^B \sigma(h_{\theta_\ell}(x_i))_{b,c}$  given in Eq. (15), we have that

$$\begin{aligned} & \|\bar{\sigma}_{\theta,\ell}(x_i)_c - \bar{\sigma}_{\theta',\ell}(x_i)_c\| \\ & = \left\| \frac{1}{B} \sum_{b=1}^B (\sigma(h_{\theta_\ell}(x_i))_{b,c} - \sigma(h_{\theta'_\ell}(x_i))_{b,c}) \right\| \\ & \leq \frac{1}{B} \sum_{b=1}^B \|\sigma(h_{\theta_\ell}(x_i))_{b,c} - \sigma(h_{\theta'_\ell}(x_i))_{b,c}\|, \end{aligned} \quad (36)$$

in which we used the triangle inequality. Thus, we must establish Lipschitz continuity of  $\sigma(h_{\theta_\ell}(x_i))_{b,c}$ . Towards this, we first use the difference of squares rule to obtain

$$\begin{aligned} & \|\sigma(h_{\theta_\ell}(x_i))_{b,c} - \sigma(h_{\theta'_\ell}(x_i))_{b,c}\| \\ & = \frac{\|\sigma^2(h_{\theta_\ell}(x_i))_{b,c} - \sigma^2(h_{\theta'_\ell}(x_i))_{b,c}\|}{\|\sigma(h_{\theta_\ell}(x_i))_{b,c} + \sigma(h_{\theta'_\ell}(x_i))_{b,c}\|} \\ & \geq \frac{\|\sigma^2(h_{\theta_\ell}(x_i))_{b,c} - \sigma^2(h_{\theta'_\ell}(x_i))_{b,c}\|}{\min_{\theta_\ell, x_i} \{\|\sigma(h_{\theta_\ell}(x_i))_{b,c}\|\}} \\ & \geq \frac{1}{\sqrt{\eta}} \|\sigma^2(h_{\theta_\ell}(x_i))_{b,c} - \sigma^2(h_{\theta'_\ell}(x_i))_{b,c}\|, \end{aligned} \quad (37)$$

where we used the fact that  $\sigma(\cdot)_{b,c} > 0$  is always non-negative, and then invoked the lower bound of Eq. (26). Similar to before, we must establish Lipschitz continuity of

$\sigma^2(h_{\theta_\ell}(x_i))_{b,c}$  to prove Eq. (37) (and in turn of Eq. (36)). Using the definition of the function  $\sigma^2(\cdot)_{b,c}$  in Eq. (2), we have that

$$\begin{aligned} & \sigma^2(h_{\theta_\ell}(x_i))_{b,c} \\ & = \frac{1}{HW} \sum_{h=1}^H \sum_{w=1}^W (h_{\theta_\ell}(x_i)_{b,c,h,w} - \mu(h_{\theta_\ell}(x_i))_{b,c})^2 + \eta \\ & = \frac{1}{HW} \sum_{h=1}^H \sum_{w=1}^W h_{\theta_\ell}(x_i)_{b,c,h,w}^2 - \mu(h_{\theta_\ell}(x_i))_{b,c}^2 + \eta. \end{aligned} \quad (38)$$

Thus, we can obtain the following for the last term in Eq. (37)

$$\begin{aligned} & \|\sigma^2(h_{\theta_\ell}(x_i))_{b,c} - \sigma^2(h_{\theta'_\ell}(x_i))_{b,c}\| \\ & = \left\| \frac{1}{HW} \sum_{h=1}^H \sum_{w=1}^W (h_{\theta_\ell}(x_i)_{b,c,h,w}^2 - h_{\theta'_\ell}(x_i)_{b,c,h,w}^2) \right. \\ & \quad \left. - (\mu(h_{\theta_\ell}(x_i))_{b,c}^2 - \mu(h_{\theta'_\ell}(x_i))_{b,c}^2) \right\| \\ & \leq \frac{1}{HW} \sum_{h=1}^H \sum_{w=1}^W \|h_{\theta_\ell}(x_i)_{b,c,h,w}^2 - h_{\theta'_\ell}(x_i)_{b,c,h,w}^2\| \\ & \quad + \|\mu(h_{\theta_\ell}(x_i))_{b,c}^2 - \mu(h_{\theta'_\ell}(x_i))_{b,c}^2\|, \end{aligned} \quad (39)$$

in which we used the triangle inequality. To bound Eq. (39), we focus on its constituents. We first have that

$$\begin{aligned} & \|h_{\theta_\ell}(x_i)_{b,c,h,w}^2 - h_{\theta'_\ell}(x_i)_{b,c,h,w}^2\| \\ & = \|h_{\theta_\ell}(x_i)_{b,c,h,w} + h_{\theta'_\ell}(x_i)_{b,c,h,w}\| \\ & \quad \|h_{\theta_\ell}(x_i)_{b,c,h,w} - h_{\theta'_\ell}(x_i)_{b,c,h,w}\| \\ & \leq 2 \max_{\theta_\ell} \{\|h_{\theta_\ell}(x_i)_{b,c,h,w}\|\} D_{i,\ell} \|\theta - \theta'\| \\ & = 2U_i D_{i,\ell} \|\theta - \theta'\|, \end{aligned} \quad (40)$$

where we used the difference of squares formula, and then invoked Assumption 5.3-(a) and 5.3-(b). For the second term in Eq. (39), we have

$$\begin{aligned} & \|\mu(h_{\theta_\ell}(x_i))_{b,c}^2 - \mu(h_{\theta'_\ell}(x_i))_{b,c}^2\| \\ & = \|\mu(h_{\theta_\ell}(x_i))_{b,c} + \mu(h_{\theta'_\ell}(x_i))_{b,c}\| \\ & \quad \|\mu(h_{\theta_\ell}(x_i))_{b,c} - \mu(h_{\theta'_\ell}(x_i))_{b,c}\| \\ & \leq 2 \max_{\theta_\ell} \{\|\mu(h_{\theta_\ell}(x_i))_{b,c}\|\} D_{i,\ell} \|\theta - \theta'\| \\ & = 2U_i D_{i,\ell} \|\theta - \theta'\|, \end{aligned} \quad (41)$$

where we used the difference of squares formula, and then invoked the results of Lemma A.1-(a) and Proposition 5.4-(a). Putting Eqs. (40) and (41) together and plugging them back in (39), and then we get

$$\begin{aligned} & \|\sigma^2(h_{\theta_\ell}(x_i))_{b,c} - \sigma^2(h_{\theta'_\ell}(x_i))_{b,c}\| \\ & \leq \frac{1}{HW} \sum_{h=1}^H \sum_{w=1}^W 2U_{i,\ell} D_{i,\ell} \|\theta - \theta'\| + 2U_i D_{i,\ell} \|\theta - \theta'\| \\ & = 4U_i D_{i,\ell} \|\theta - \theta'\|. \end{aligned} \quad (42)$$

Finally, we employ Eq. (42) in Eq. (37) followed by Eq. (36) to get

$$\begin{aligned} \|\bar{\sigma}_{\theta,\ell}(x_i)_c - \bar{\sigma}_{\theta',\ell}(x_i)_c\| &\leq \frac{1}{B} \sum_{b=1}^B \frac{4U_i D_{i,\ell}}{\sqrt{\eta}} \|\theta - \theta'\| \\ &= \frac{4U_i D_{i,\ell}}{\sqrt{\eta}} \|\theta - \theta'\|. \end{aligned} \quad (43)$$

*Proof A.8:* (c) Using the definition  $\Sigma_{\mu,\theta,\ell}^2(x_i)_c = \Sigma_{\mu}^2(h_{\theta_\ell}(x_i))_c$  given in Eq. (15) and the definition of the function  $\Sigma_{\mu}^2(\cdot)_c$  in Eq. (3), we have that

$$\begin{aligned} \Sigma_{\mu,\theta,\ell}^2(x_i)_c &= \frac{1}{B} \sum_{b=1}^B (\mu(h_{\theta_\ell}(x_i))_{b,c} - \mathbb{E}_b[\mu(h_{\theta_\ell}(x_i))_{b,c}])^2 + \eta \\ &= \frac{1}{B} \sum_{b=1}^B \mu(h_{\theta_\ell}(x_i))_{b,c}^2 - \bar{\mu}_{\theta,\ell}(x_i)_c^2 + \eta, \end{aligned} \quad (44)$$

where we used the definition of  $\bar{\mu}_{\theta,\ell}(x_i)_c$  from Eq. (15). Consequently, we can obtain the bound

$$\begin{aligned} \|\Sigma_{\mu,\theta,\ell}^2(x_i)_c - \Sigma_{\mu,\theta',\ell}^2(x_i)_c\| &= \left\| \frac{1}{B} \sum_{b=1}^B (\mu(h_{\theta_\ell}(x_i))_{b,c}^2 - \mu(h_{\theta'_\ell}(x_i))_{b,c}^2) \right. \\ &\quad \left. - (\bar{\mu}_{\theta,\ell}(x_i)_c^2 - \bar{\mu}_{\theta',\ell}(x_i)_c^2) \right\| \\ &\leq \frac{1}{B} \sum_{b=1}^B \|\mu(h_{\theta_\ell}(x_i))_{b,c}^2 - \mu(h_{\theta'_\ell}(x_i))_{b,c}^2\| \\ &\quad + \|\bar{\mu}_{\theta,\ell}(x_i)_c^2 - \bar{\mu}_{\theta',\ell}(x_i)_c^2\|, \end{aligned} \quad (45)$$

in which we used the triangle inequality. We have obtained a bound for the first term of Eq. (45) in Eq. (41), and we focus on the second term next. We have that

$$\begin{aligned} \|\bar{\mu}_{\theta,\ell}(x_i)_c^2 - \bar{\mu}_{\theta',\ell}(x_i)_c^2\| &= \|\bar{\mu}_{\theta,\ell}(x_i)_c + \bar{\mu}_{\theta',\ell}(x_i)_c\| \|\bar{\mu}_{\theta,\ell}(x_i)_c - \bar{\mu}_{\theta',\ell}(x_i)_c\| \\ &\leq 2 \max_{\theta,\ell} \{\|\bar{\mu}_{\theta,\ell}(x_i)_c\|\} D_{i,\ell} \|\theta - \theta'\| \\ &= 2U_i D_{i,\ell} \|\theta - \theta'\|, \end{aligned} \quad (46)$$

where we used the difference of squares law, and then invoke the results of Lemma A.1-(c) and Proposition 5.4-(a), respectively. To conclude the proof, we plug back Eqs. (46) and (41) back in Eq. (45) to get

$$\begin{aligned} \|\Sigma_{\mu,\theta,\ell}^2(x_i)_c - \Sigma_{\mu,\theta',\ell}^2(x_i)_c\| &\leq \frac{1}{B} \sum_{b=1}^B 2U_i D_{i,\ell} \|\theta - \theta'\| + 2U_i D_{i,\ell} \|\theta - \theta'\| \\ &= 4U_i D_{i,\ell} \|\theta - \theta'\|. \end{aligned} \quad (47)$$

*Proof A.9:* (d) Using the definition  $\Sigma_{\sigma,\theta,\ell}^2(x_i)_c = \Sigma_{\sigma}^2(h_{\theta_\ell}(x_i))_c$  given in Eq. (15) and the definition of the function  $\Sigma_{\sigma}^2(\cdot)_c$  in Eq. (3), we have that

$$\begin{aligned} \Sigma_{\sigma,\theta,\ell}^2(x_i)_c &= \frac{1}{B} \sum_{b=1}^B (\sigma(h_{\theta_\ell}(x_i))_{b,c} - \mathbb{E}_b[\sigma(h_{\theta_\ell}(x_i))_{b,c}])^2 + \eta \\ &= \frac{1}{B} \sum_{b=1}^B \sigma(h_{\theta_\ell}(x_i))_{b,c}^2 - \bar{\sigma}_{\theta,\ell}^2(x_i)_c + \eta, \end{aligned} \quad (48)$$

where we used the definition of  $\bar{\sigma}_{\theta,\ell}^2(x_i)_c$  from Eq. (15). Hence, we can obtain the bound

$$\begin{aligned} \|\Sigma_{\sigma,\theta,\ell}^2(x_i)_c - \Sigma_{\sigma,\theta',\ell}^2(x_i)_c\| &= \left\| \frac{1}{B} \sum_{b=1}^B (\sigma(h_{\theta_\ell}(x_i))_{b,c}^2 - \sigma(h_{\theta'_\ell}(x_i))_{b,c}^2) \right. \\ &\quad \left. - (\bar{\sigma}_{\theta,\ell}^2(x_i)_c - \bar{\sigma}_{\theta',\ell}^2(x_i)_c) \right\| \\ &\leq \frac{1}{B} \sum_{b=1}^B \|\sigma(h_{\theta_\ell}(x_i))_{b,c}^2 - \sigma(h_{\theta'_\ell}(x_i))_{b,c}^2\| \\ &\quad + \|\bar{\sigma}_{\theta,\ell}^2(x_i)_c - \bar{\sigma}_{\theta',\ell}^2(x_i)_c\|, \end{aligned} \quad (49)$$

in which we used the triangle inequality. We have obtained bounds for the first term of Eq. (49) in Eq. (42), and we focus on the second term next. We have that

$$\begin{aligned} \|\bar{\sigma}_{\theta,\ell}(x_i)_c^2 - \bar{\sigma}_{\theta',\ell}(x_i)_c^2\| &= \|\bar{\sigma}_{\theta,\ell}(x_i)_c + \bar{\sigma}_{\theta',\ell}(x_i)_c\| \|\bar{\sigma}_{\theta,\ell}(x_i)_c - \bar{\sigma}_{\theta',\ell}(x_i)_c\| \\ &\leq 2 \max_{\theta,\ell} \{\|\bar{\sigma}_{\theta,\ell}(x_i)_c\|\} \frac{4U_i D_{i,\ell}}{\sqrt{\eta}} \|\theta - \theta'\| \\ &= \frac{8\sqrt{2}U_i^2 D_{i,\ell}}{\sqrt{\eta}} \|\theta - \theta'\|, \end{aligned} \quad (50)$$

where we used the difference of squares law, and then invoke the results of Lemma A.1-(d) and Proposition 5.4-(b), respectively. To conclude the proof, we plug back Eqs. (50) and (42) back in Eq. (45) to get

$$\begin{aligned} \|\Sigma_{\sigma,\theta,\ell}^2(x_i)_c - \Sigma_{\sigma,\theta',\ell}^2(x_i)_c\| &\leq \frac{1}{B} \sum_{b=1}^B 4U_i D_{i,\ell} \|\theta - \theta'\| + \frac{8\sqrt{2}U_i^2 D_{i,\ell}}{\sqrt{\eta}} \|\theta - \theta'\| \\ &= 4U_i D_{i,\ell} \left( 1 + \frac{2\sqrt{2}U_i}{\sqrt{\eta}} \right) \|\theta - \theta'\|. \end{aligned} \quad (51)$$

*Proof A.10:* With the bounds for all 4 individual style statistics of each device  $i \in \mathcal{M}$  at a given layer/block  $\ell = \{1, \dots, L\}$  derived in Proposition 5.4, we move on to analyze the Lipschitz continuity of  $\psi_{\theta,\ell}(x_i) = [\bar{\mu}_{\theta,\ell}(x_i) \quad \bar{\sigma}_{\theta,\ell}(x_i) \quad \Sigma_{\mu,\theta,\ell}^2(x_i) \quad \Sigma_{\sigma,\theta,\ell}^2(x_i)]^T$ , which is a

vector concatenating all of them for a single client  $i$  at a single layer  $\ell$ . We have

$$\begin{aligned}
& \|\psi_{\theta,\ell}(x_i) - \psi_{\theta',\ell}(x_i)\| \\
& \leq \|\bar{\mu}_{\theta,\ell}(x_i) - \bar{\mu}_{\theta',\ell}(x_i)\| + \|\bar{\sigma}_{\theta,\ell}(x_i) - \bar{\sigma}_{\theta',\ell}(x_i)\| \\
& \quad + \|\Sigma_{\mu,\theta,\ell}^2(x_i) - \Sigma_{\mu,\theta',\ell}^2(x_i)\| + \|\Sigma_{\sigma,\theta,\ell}^2(x_i) - \Sigma_{\sigma,\theta',\ell}^2(x_i)\| \\
& \leq \left( D_{i,\ell} + \frac{4U_i D_{i,\ell}}{\sqrt{\eta}} + 4U_i D_{i,\ell} + 4U_i D_{i,\ell} \left( 1 + \frac{2\sqrt{2}U_i}{\sqrt{\eta}} \right) \right) \|\theta - \theta'\| \\
& = \left( 1 + 4U_i \left( 1/\sqrt{\eta} + 2 + (2\sqrt{2}U_i)/\sqrt{\eta} \right) \right) D_{i,\ell} \|\theta - \theta'\|, \tag{52}
\end{aligned}$$

in which we used the triangle inequality. Next, we focus on  $\psi_{\theta}(x_i) = [\psi_{\theta,1}(x_i) \ \cdots \ \psi_{\theta,L}(x_i)]^T$ , which is a vector concatenating the style statistics across all the layers of the CNN for a given client  $i \in \mathcal{M}$ . We have that

$$\begin{aligned}
\|\psi_{\theta}(x_i) - \psi_{\theta'}(x_i)\| & \leq \sum_{\ell=1}^L \|\psi_{\theta,\ell}(x_i) - \psi_{\theta',\ell}(x_i)\| \\
& \leq L \left( 1 + 4U_i \left( 1/\sqrt{\eta} + 2 + (2\sqrt{2}U_i)/\sqrt{\eta} \right) \right) D_i \|\theta - \theta'\|, \tag{53}
\end{aligned}$$

in which we used the triangle inequality. Finally, the Lipschitzness of  $\Psi_{\theta}(X) = [\psi_{\theta}(x_1) \ \cdots \ \psi_{\theta}(x_m)]^T$  follows similarly as

$$\begin{aligned}
\|\Psi_{\theta}(X) - \Psi_{\theta'}(X)\| & \leq \sum_{i=1}^m \|\psi_{\theta}(x_i) - \psi_{\theta'}(x_i)\| \\
& \leq mL \left( 1 + 4U \left( 1/\sqrt{\eta} + 2 + (2\sqrt{2}U)/\sqrt{\eta} \right) \right) D \|\theta - \theta'\|, \tag{54}
\end{aligned}$$

in which we used the triangle inequality, and  $m$  is the total number of devices in the decentralized network. Noting that  $\Psi_{\theta_i}(X) \subset \Psi_{\theta}(X)$ , we thus have that

$$\begin{aligned}
& \|\Psi_{\theta,i}(X) - \Psi_{\theta',i}(X)\| \\
& \leq mL \left( 1 + 4U \left( 1/\sqrt{\eta} + 2 + (2\sqrt{2}U)/\sqrt{\eta} \right) \right) D \|\theta - \theta'\|. \tag{55}
\end{aligned}$$

Plugging the last equation above into Assumption 5.1, we obtain

$$\begin{aligned}
& \|\nabla F_i(\theta, \Psi_{\theta,i}(X)) - \nabla F_i(\theta', \Psi_{\theta',i}(X))\| \\
& \leq \beta_{\theta,i} \|\theta - \theta'\| + \beta_{\Psi,i} \|\Psi_{\theta,i}(X) - \Psi_{\theta',i}(X)\| \\
& \leq \left[ \beta_{\theta,i} + mL \left( 1 + 4U \left( 1/\sqrt{\eta} + 2 + (2\sqrt{2}U)/\sqrt{\eta} \right) \right) \right. \\
& \quad \left. D\beta_{\Psi,i} \right] \|\theta - \theta'\|. \tag{56}
\end{aligned}$$